IEEE Photonics Journal
An IEEE Photonics Society Publication

Open Access

Effect of Phase Relations on Speckle Pattern: Simulation and Measurement

Volume 11, Number 4, August 2019

Linlu He
Haitao Zhang
Decai Deng
Qihang Gong
Jiaqi Zu
Kuo Meng

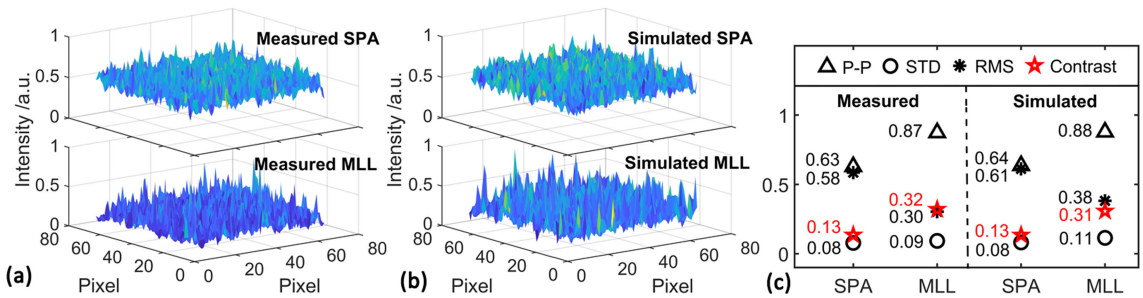

DOI: 10.1109/JPHOT.2019.2919240
1943-0655

Effect of Phase Relations on Speckle Pattern: Simulation and Measurement

Linlu He,[1] Haitao Zhang,[1] Decai Deng,[1] Qihang Gong,[1] Jiaqi Zu,[1] and Kuo Meng[2]

[1]Center for Photonics and Electronics, Department of Precision Instruments, Tsinghua University, Beijing 100084, China
[2]Engineering Research Center of Optoelectronics Information and Instrument, Beijing Key Laboratory of Optoelectronic Measurement Technology, Beijing Laboratory for Biomedical Detection Technology and Instrument, Beijing Information Science and Technology University, Beijing 100192, China

DOI:10.1109/JPHOT.2019.2919240

Manuscript received March 18, 2019; revised May 19, 2019; accepted May 21, 2019. Date of publication May 28, 2019; date of current version June 28, 2019. This work was supported in part by Beijing Natural Science Foundation (4184087), in part by the National Natural Science Foundation of China (61475081), and in part by Sichuan Province Science and Technology Support Program (2018JZ0015).
Corresponding author: Haitao Zhang (e-mail: zhanghaitao@mail.tsinghua.edu.cn).

Abstract: Speckle is an important phenomenon in various applications. It can be quantified by speckle contrast. However, at present, the influence of the phase relations among the various wavelengths on speckle contrast is rarely analyzed theoretically. Herein, a thorough method for numerically simulating the speckle pattern is presented to considering the impact of relative phase relations among wavelengths on speckle contrast. This method contains spectral shape, spectral width, and phase relations. In addition, a superluminescent pulse amplifier (SPA) with 6.5-nm bandwidth and a mode-locked laser (MLL) with 21-nm bandwidth are established to conduct the verification experiment. The experimental results show that the SPA light attains lower speckle contrast even with a narrower bandwidth than the MLL light. It is manifested that relative phase relations among wavelengths has significant effect on speckle contrast, and chaotic phase relations could be more advantageous for reducing speckle than just a broad spectrum. The simulation results agree well with experimental results. Therefore, this thorough method could provide a reliable approach to describe the characteristics of speckle pattern caused by broadband light carrying phase information. Considering the speckle contrast is positively proportional to optical coherence, this method could also be used to analyze the coherence of partially coherent light.

Index Terms: Speckle, phase relations, coherence.

1. Introduction

With the advent of high-coherence lasers, the speckle phenomenon is observed in coherent imaging modality. Sometimes this is a desired phenomenon, e.g., in laser speckle imaging (LSI), since it provides access to physiological processes in vivo with excellent temporal and spatial resolution [1], [2]. Over the years a variety of algorithms have been developed for simulating laser speckle in LSI [3], [4], and the research on coherent laser speckle has almost matured. However, speckle phenomenon could also be a crucial problem that seriously impairs the image quality of laser based displays [5], [6]. Since the speckle is generated due to the high coherence of laser, one of the method to eliminate the speckle is to reduce the coherence of the light source, such as

using partially coherence light source [7], [8]. The speckle pattern can be quantified by the speckle contrast, which is quite important in the analysis of speckle patterns. At present, in the spectrum domain, the theoretical studies of speckle contrast are mainly limited to discuss the influence of spectral bandwidth [9]–[13]. Equation (1) shows the most commonly used formula for calculating the speckle contrast under Gaussian-shape spectrum [11]

$$C = 1/4\sqrt{1 + 8\pi^2\left(\frac{\Delta\lambda}{\lambda}\right)^2\left(\frac{\sigma_h}{\lambda}\right)}^2 \tag{1}$$

where σ_h is the standard deviation of the rough surface height fluctuates from the Gaussian distribution, λ is the central wavelength, and $\Delta\lambda$ is the spectral width. It is shown that speckle contrast C is negatively correlated with the spectral width and positively correlated with the central wavelength and the standard deviation.

In Eq. (1), we could replace the Gaussian-shape spectrum with the actual measured spectrum to get a more accurate result. However, even Eq. (1) amended with the measured spectrum shape is not accurate enough for a broadband partially light if the relative phase relations under different wavelengths is not considered. Therefore, an improved method combined spectral shape for speckle contrast simulation is in need.

In this paper, we propose a thorough method to numerically simulate three-dimensional (3-D) speckle pattern. The relative phase relations under different wavelengths as well as spectral width and shape are considered in our method. Statistical results include speckle contrast could be attained directly from the simulated speckle pattern. Moreover, we use a superluminescent pulse amplifier (SPA) with 6.5-nm bandwidth at center wavelength of 1064 nm and a mode-locked fiber laser with 21-nm bandwidth at 1030 nm to conduct verification experiments. The relative phase relations among the wavelengths of the mode-locked laser (MLL) are locked. The SPA source is constructed by a superluminescent diode (SLD) seed with nonlongitudinal mode structure and cascaded fiber amplifiers. And the phase relations under different wavelengths in its spectral range is chaotic. It is found that although the bandwidth of the MLL source is broader than that of SPA source, the former has higher speckle contrast. Therefore, the relative phase relations shows significant impact on speckle contrast, and chaotic phase relations could be more advantageous in reducing speckle than just a broad spectrum. The experimental results achieve qualitative agreement with our simulation results. Thus, this method provides a reliable approach to describe the characteristics of speckle pattern caused by broadband light carrying phase information. In addition, since the speckle contrast is positively proportional to comprehensive spatiotemporal optical coherence [14], it is possible to measure the coherence of partially coherent light with this thorough method.

2. Theory

Herein, ignoring the interference and coupling effects between different polarization modes, we could simplify the simulation of the optical coherence in one polarization state. Speckle is derived from the coherent superposition of random wavelets generated by a rough surface from a light source as shown in Fig. 1.

$U_i(x_0, y_0, \lambda)$ denotes the complex amplitudes of the light field emitted on plane x_0y_0 of scattering screen from the light source, $U_o(x_0, y_0, \lambda)$ denotes the complex amplitudes of the scattered light field distribution from scattering screen, and $U(x, y, \lambda)$ denotes the optical wave field propagating to plane xy of the observation screen after passing distance z.

Taking m photons in each wavelength into consideration, we decompose the light field distribution at a single wavelength in different photon states, which can be expressed as

$$U_i(x_0, y_0, \lambda) = \sum_m A'_m(\lambda)U_i^m(x_0, y_0, \lambda)\exp[i\varphi_m(x_0, y_0, \lambda)] \tag{2}$$

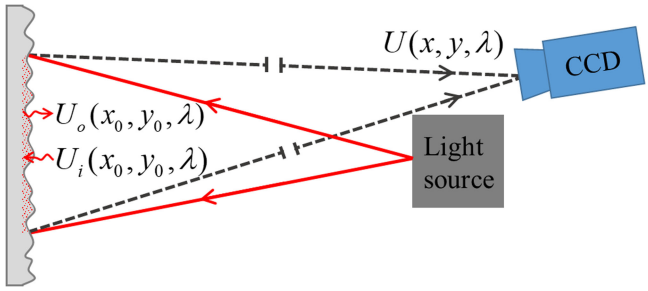

Fig. 1. Speckle measurement diagram.

where $A'_m(\lambda)$, $U_i^m(x_0, y_0, \lambda)$, and $\varphi_m(x_0, y_0, \lambda)$ represent the amplitude ratio corresponding to the spectral shape, the electric field distribution, and the phase information of photon state m with wavelength λ, respectively.

The scattered field is generated by wavelets formed on the scattering surface that are radiated at random locations with a random initial phase. In the numerical simulation, the scattered field of m-th photon can be expressed by

$$U_o^m(x_0, y_0, \lambda) = A_m(x_0, y_0, \lambda) U_i^m(x_0, y_0, \lambda) \exp[i\phi_m(x_0, y_0, \lambda)] \tag{3}$$

where $\phi_m(x_0, y_0, \lambda)$ is a random phase matrix and $A_m(x_0, y_0, \lambda)$ is a random amplitude matrix, which are both caused by m-th photon emitted on the scattering screen.

It is proved that wavelength change causes phase shift and light field variation, since the phase of the k-th scattered wave $\phi_k(x_0, y_0, \lambda) = 2\pi s_k/\lambda$ (s_k is the additional optical path length that the scattering object brings to the k-th scattered wave), which is inversely proportional to wavelength λ [15]. Wavelength change also leads to the movement of the speckle pattern because the diffraction angle $\theta_d = \rho\lambda$ (ρ is the aperture size limit), which is positively proportional to wavelength λ. The phase shift $\phi_k(x_0, y_0, \lambda)$ could be considered as an additional phase factor corresponding to the spectrum of the light source in the phase matrix $\phi_m(x_0, y_0, \lambda)$. The diffraction angle θ_d could cause the movement of speckle pattern. In the simulation, it means that the element in the amplitude matrix $A_m(x_0, y_0, \lambda)$ will move relates to the wavelength. This effect would be contained into the amplitude matrix $A_m(x_0, y_0, \lambda)$ in our simulation.

Therefore, the thorough scattered field $U_o(x_0, y_0, \lambda)$ at single wavelength can be expressed as

$$U_o(x_0, y_0, \lambda) = \sum_m A_m(x_0, y_0, \lambda) A'_m(\lambda) U_i^m(x_0, y_0, \lambda) \exp[2\pi i \cdot 2h(x_0, y_0)/\lambda + i\varphi_m(x_0, y_0, \lambda)] \tag{4}$$

where $h(x_0, y_0)$ is a wavelength-independent random height matrix of scattering screen and $2h$ (x_0, y_0) denote the optical path length produced by scattering screen at position (x_0, y_0).$\varphi_m(x_0, y_0, \lambda)$ is a phase matrix relates to the relative phase relations among wavelengths.

According to angle-spectrum diffraction theory, the relationship between the complex amplitudes of the optical wave field from the scattering screen to the observation screen in the Fraunhofer diffraction zone can be expressed by

$$U(x, y, \lambda) = \mathscr{F}^{-1}\left\{\mathscr{F}\{U_o(x_0, y_0, \lambda)\} \exp\left[i\frac{2\pi}{\lambda} z\sqrt{1 - (\lambda f_x)^2 - (\lambda f_y)^2}\right]\right\} \tag{5}$$

where $\mathscr{F}\{\}$ denotes the spatial Fourier transform.

The speckle generated by the broadband light can be considered a sum of single-frequency light-generating speckles since different wavelengths cannot be coherently superimposed.

$$U(x, y) = \int_0^\infty U(x, y, \lambda) d\lambda \tag{6}$$

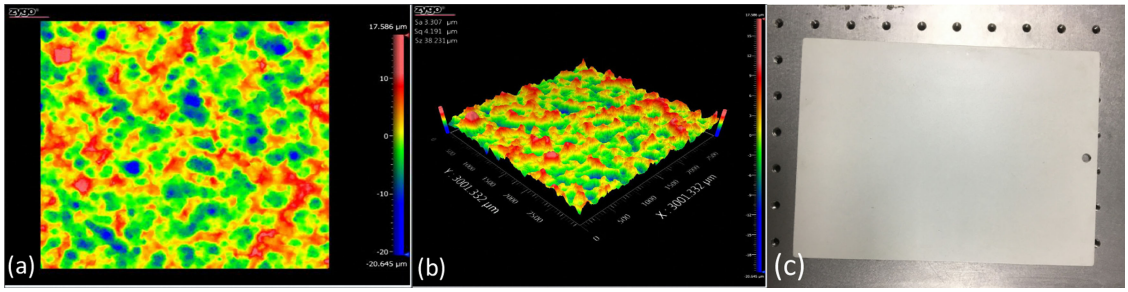

Fig. 2. Surface structure diagram. (a) Two-dimensional image. (b) Three-dimensional image. (c) Its photo.

By substituting Eqs. (4) and (5) into Eq. (6), we can obtain Eq. (7) as the complex amplitudes of the light wave distribution on the observation plane xy. This is the final formula used to simulate 3-D speckle pattern.

$$U(x,y) = \int_0^\infty \mathscr{F}^{-1}\left\{\mathscr{F}\left\{\sum_m A_m(x_0,y_0,\lambda)A'_m(\lambda)U_i^m(x_0,y_0,\lambda)\exp[2\pi i\cdot 2h(x_0,y_0)/\lambda + i\varphi_m(x_0,y_0,\lambda)]\right\}\right.$$
$$\left.\times \exp\left[i\frac{2\pi}{\lambda}z\sqrt{1-(\lambda f_x)^2-(\lambda f_y)^2}\right]\right\} d\lambda * H \tag{7}$$

A CCD will be used to collect speckle patterns. Due to the influence of light intensity, a single light point may expand to a small bright spot when received on the CCD. Therefore, the response of CCD should be considered as well. The last parameter H in Eq. (7) represents an adjustable response matrix of the CCD. This response matrix H is used to reflect this change from a light point to the bright spot.

The random height matrix $h(x_0, y_0)$ could derive from the real viewing screen used in the experiment. However, since it is difficult to define the random factors directly, the two matrixes $\varphi_m(x_0, y_0, \lambda)$ and $A_m(x_0, y_0, \lambda)$ are adjustable. It is worth noting that since the diffraction angle is positively proportional to the wavelength, the elements in $A_m(x_0, y_0, \lambda)$ will move according to the change in wavelength. This amplitude matrix for each wavelength is not completely random.

3. Simulation and Experiment

The random height matrix $h(x_0, y_0)$ for our simulation is derived from a coarse white metal viewing screen used in the experiment and measured by surface topography. As shown in Fig. 2, its arithmetical mean height $S_a = 3.307\ \mu$m, root mean square deviation $S_q = 4.191\ \mu$m and maximum height of profile $S_z = 38.231\ \mu$m.

To compare the coherence of light with the locked and chaotic phase relationship, we construct two light sources. The first is the SPA system mentioned in Ref. [16]. The second is an MLL with the seed source mentioned in Ref. [17] and amplified according to the theory mentioned in Ref. [18]. The original spectra of these two light sources are manifested in Fig. 3(a). The SPA light attains 6.5-nm bandwidth at central wavelength of 1062 nm, and the MLL light attains 21-nm bandwidth at 1031 nm. Then, we use filters to limit the spectral width of both light sources to 3 nm, and the limited spectra are given in Fig. 3(b). Based on these two light sources, we can numerically simulate and experimentally verify the effect of spectral width and phase information on optical coherence.

Figure 4 shows the measured and simulated speckle patterns of SPA and MLL light without filters. The diffuse reflected light of the white metal viewing screen which is shown in Fig. 2 is received by the CCD to form speckle patterns.

The measured speckle patterns are shown in Fig. 4(a) and Fig. 4(b). Meanwhile, the numerically simulated speckle patterns of SPA and MLL light can be obtained by substituting the spectra in

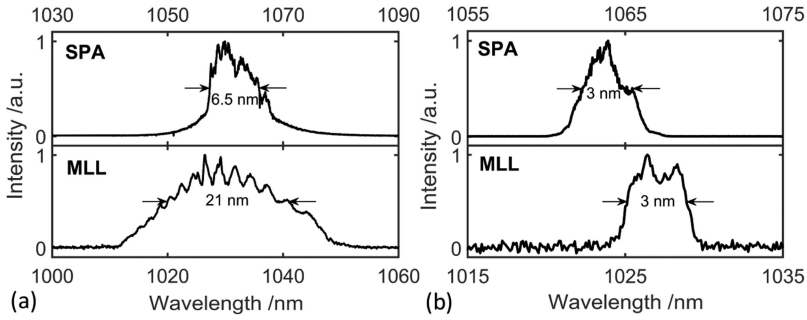

Fig. 3. Spectra of SPA (top row on each panel) and MLL (bottom row). (a) Without filters. (b) With filters.

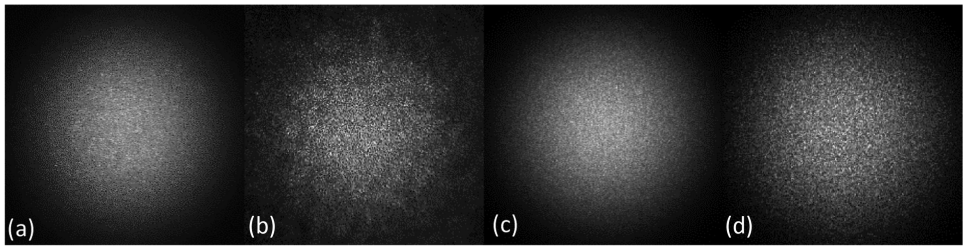

Fig. 4. Measured speckle patterns. (a) SPA. (b) MLL; Simulated speckle patterns. (c) SPA. (d) MLL. (Without filters).

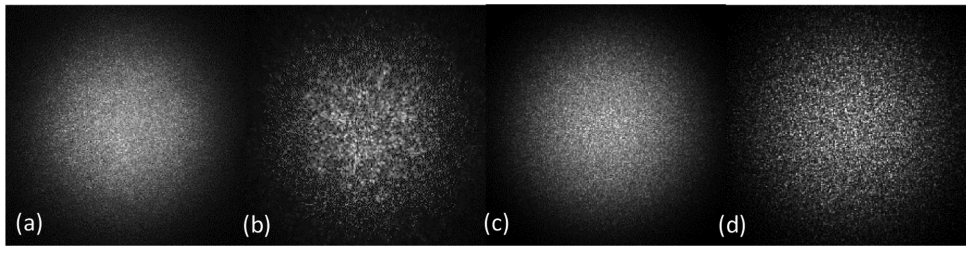

Fig. 5. Measured speckle patterns. (a) SPA. (b) MLL; Simulated speckle patterns. (c) SPA. (d) MLL. (With filters).

Fig. 3(a) and the measured surface height parameter into Eq. (7). The simulated speckle patterns are given in Fig. 4(c) and Fig. 4(d) for comparison.

Furthermore, the simulated and measured speckle patterns of SPA and MLL light with filters are shown in Fig. 5.

It can be determined from Figs. 4 and 5 that the speckle patterns of SPA light seem smoother and the noise size seems smaller than the speckle pattern of MLL light. Moreover, the simulated speckle patterns are in good agreement with the measured speckle patterns. These results indicate that our method achieves qualitative agreement with the experiments. We could obtain the speckle characteristics through its statistical results clearly.

When obtaining the speckle contrast C from the speckle pattern directly, it can be expressed as

$$C = \frac{\sigma_1}{\bar{I}} = \frac{\sqrt{\overline{I(x,y)^2} - [\overline{I(x,y)}]^2}}{\overline{I(x,y)}} \tag{8}$$

where $I(x, y)$ is the light intensity of the speckle pattern on plane xy and σ_1 is the standard deviation of light intensity.

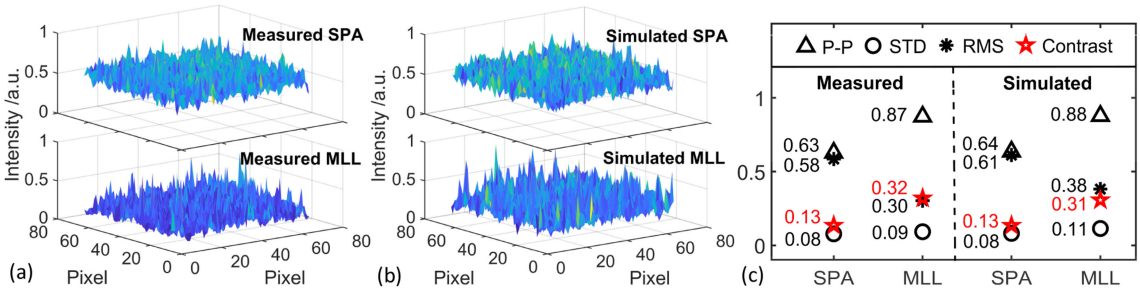

Fig. 6. (a) Simulated speckle intensities. (b) Measured speckle intensities of SPA (top row on each panel) and MLL (bottom row). (c) Statistical results. (Without filters). P-P, peak-to-peak value; STD, standard deviation; RMS, root mean square; Contrast, speckle contrast.

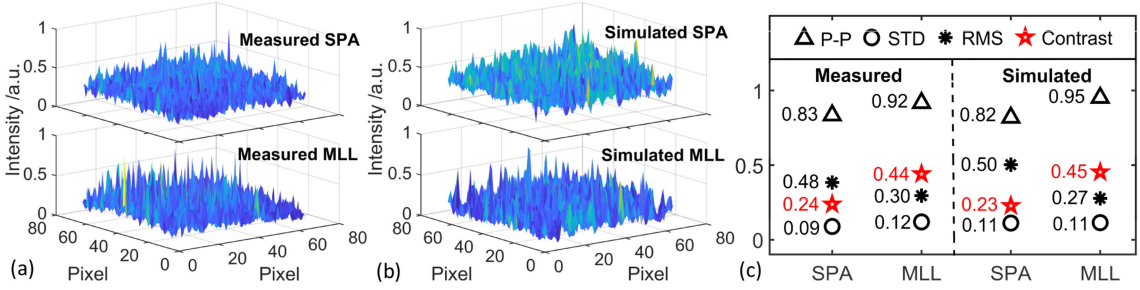

Fig. 7. (a) Measured speckle intensities. (b) Simulated speckle intensities of SPA (top row on each panel) and MLL (bottom row). (c) Statistical results of SPA and MLL. (With filters).

To reduce the impact of the surrounding light, we adopt 64 $*$ 64-pixel small piece in each speckle pattern to calculate the statistical results, including speckle contrasts. The results for SPA and MLL light without filters are shown in Fig. 6. Figure 6(a) and (b) show the measured and simulated light intensity of selected small pieces, respectively. Figure 6(c) shows the statistical results include peak-to-peak value, standard deviation, root mean square, and speckle contrast of measured and simulated speckle patterns.

Figure 6 manifests that in the case without filters, the measured speckle contrast of SPA is 0.13, which is nearly 1/3 of the speckle contrast of the MLL (0.32). We can infer that SPA light speckle has a smoother structure. The chaotic phase relations produces more cluttered scattering fields which smooths its structure. As a result, the speckle caused by the SPA source attains lower speckle contrast.

The lower speckle contrast of the SPA source in both cases indicates lower optical coherence. Therefore, we can infer that the coherence of an SPA source with 6.5-nm bandwidth is lower than that of an MLL source with 21-nm bandwidth. This result shows that the phase relationship has a significant impact on speckle contrast and optical coherence. The chaotic phase relations could be more advantageous in reducing coherence than just a broad spectrum.

Figure 7 manifests the simulated and measured speckle intensities and statistical results of SPA and MLL light with filters. When the spectra of the two light sources are both limited to 3 nm, the speckle contrast rises to 0.24 for SPA and 0.44 for the MLL light. The lower speckle contrast also indicates lower coherence for SPA light.

The experimental results are all compared with the simulated results in two cases. In the case without filters, our simulated speckle contrasts are respectively 0.13 and 0.31 for SPA and MLL light (0.13 and 0.32 in the experiment). Meanwhile, the simulated speckle contrasts with filters are 0.23 and 0.45, respectively (0.24 and 0.44 in the experiment). The similar statistical results indicate that

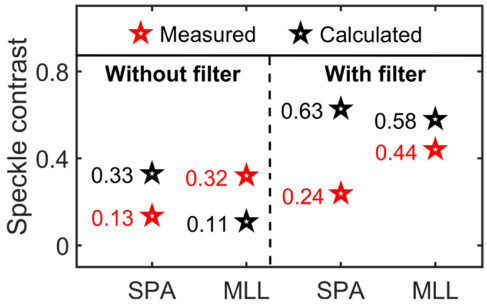

Fig. 8. Calculated and measured speckle contrast.

the 3-D speckle patterns obtained from our numerical simulation achieve qualitative agreement with the experimental results in both cases with and without filters.

The calculated speckle contrasts with Eq. (1) using the actual measured spectra in the cases with and without filters are shown in Fig. 8 comparing to measured results. Significant error exists between them. The calculated speckle contrast is obviously positively proportional to the spectral width, while the measured speckle contrast is affected by the phase relations more seriously.

Therefore, due the consideration of spectral width, spectral shape and phase information, our method could obtain more accurate results for speckle contrast when considering broadband light carrying phase information. Considering the speckle contrast is positively proportional to optical coherence, this thorough method could also be used to analyze the coherence of partially coherent light.

Figure 8 also shows a significant error between the speckle contrasts with and without filters for both two light sources. This error comes from the effect of different wavelengths on speckle pattern. It is proved that the wavelength change could cause a phase shift $\phi_k = 2\pi s_k/\lambda$ and a diffraction angle shift $\theta_d = \rho\lambda$ [15], which also have been considered in our simulation. The phase shift ϕ_k is inversely proportional to wavelength and diffraction angle θ_d is positively proportional to wavelength. It means that when the wavelength varies, it will correspond to a certain range of phase shift and diffraction angle variations. The speckle of a broadband light source could be regarded as a superposition of speckles produced by a plurality of monochromatic light. Thus for a broadband light source, the varying phase shift superimposed on the phase information will smooth the chaos of phase. Meanwhile, the diffraction angle will causes the movement of speckle pattern. A longer wavelength corresponding to a more significant movement since the diffraction angle is positively proportional to wavelength. Therefore, for a broadband light source, the varying diffraction angle superimposed on the speckle will smooth its amplitude. Considering that different wavelengths could homogenize the speckle to a certain extent, a narrow spectral light source will have a weaker homogenization effect on the speckle than a broad spectrum light source due to the narrower wavelength range. This weaker homogenization effect causes the higher speckle contrast for narrow bandwidth light source. The bandwidths of both two light sources after adding the filters are significantly reduced, so higher speckle contrasts are observed with filters.

Moreover, from the measured results of Fig. 8 we can clearly observe that the speckle contrast of SPA is lower than that of MLL no matter with or without filters. The chaotic phase relations among the wavelengths of SPA enhances the chaos of speckle field's phase and amplitude. It is equivalent to a superposition of speckles produced by a large number of beams with different phases. This superposition effect reduces the speckle contrast of SPA to some extent. Therefore, the degree of chaos in the phase relations is inversely proportional to the speckle contrast. Light source with locked phase relations will produce a higher speckle contrast while the chaotic phase relations will produce a relatively lower speckle contrast.

4. Conclusions

In summary, we have presented a thorough method combine spectral width, spectral shape and relative phase relations among wavelengths to numerically simulate speckle pattern caused by partially coherent light. In addition, we utilized two light sources, i.e., an MLL and an SPA, to analyze and verify the speckle pattern under the case of locked and chaotic phase relations. It is proved that the speckle contrast of SPA light is lower than MLL light even when the former has a narrower bandwidth (6.5 nm for SPA light and 21 nm for MLL light). Our results indicate that chaotic phase relations among the wavelengths is more conductive to get a smoother speckle pattern and a lower speckle contrast. The experiment results are in qualitative agreement with our simulation results, while the results without considering phase relations attain significant error. This comparison shows that our method is a reliable solution for simulate the speckle pattern caused by broadband light source carrying phase information. Since the speckle contrast is positively proportional to optical coherence, it is also possible to analyze the coherence of partially coherent light through this method.

References

[1] H. Cheng *et al.*, "Modified laser speckle imaging method with improved spatial resolution," *J. Biomed. Opt.*, vol. 8, no. 3, pp. 559–564, 2003.
[2] H. Cheng *et al.*, "Laser speckle imaging of blood flow in microcirculation," *Phys. Med. Biol.*, vol. 49, no. 7, pp. 1347–1357, 2004.
[3] Z. Pavel *et al.*, "Quantitative modeling of laser speckle imaging," *Opt. Lett.*, vol. 31, no. 23, pp. 3465–3467, 2006.
[4] C. Haiying and T. Q. Duong, "Simplified laser-speckle-imaging analysis method and its application to retinal blood flow imaging," *Opt. Lett.*, vol. 32, no. 15, pp. 2188–2190, 2007.
[5] M. N. Akram *et al.*, "Laser speckle reduction using a dynamic polymer-based diffraction grating spatial phase modulator," *Proc. SPIE*, vol. 7382, 2009, Art. no. 73822H.
[6] J. I. Trisnadi, "Speckle contrast reduction in laser projection displays," *Proc SPIE*, vol. 4657, no. 4657, pp. 131–137, 2002.
[7] B. Redding, M. A. Choma, and H. Cao, "Speckle-free laser imaging using random laser illumination," *Nature Photon.*, vol. 6, no. 6, pp. 355–359, 2012.
[8] A. Seungdo *et al.*, "Speckle suppression in laser display using several partially coherent beams," *Opt. Exp.*, vol. 17, 1, pp. 92–103, 2009.
[9] J. M. Huntley, "Simple model for image-plane polychromatic speckle contrast," *Appl. Opt.*, vol. 38, no. 11, pp. 2212–2215, 1999.
[10] N. A. Mansour *et al.*, "Dependence of speckle contrast on the light spectral broadening and the roughness root mean square," *Optik - Int. J. Light Electron Opt.*, vol. 133, pp. 140–149, 2017.
[11] J. W. Goodman, "Speckle phenomena in optics: Theory and applications," *J. Statistical Phys.*, vol. 130, no. 2, pp. 413–413, 2008.
[12] V. Nascov, C. Samoilă, and D. Ursuţiu, "Fast computation algorithms for speckle pattern simulation," in *Proc. AIP Conf. Amer. Inst. Phys.*, 2013, pp. 217–222.
[13] W. F. Hsu, C. F. Yeh, and M. C. Chou, "Simulation and measurement of laser speckle and speckle contrast," in *Proc. Sid Symp. Dig. Tech. Papers*, 2012, vol. 43, no. 1, pp. 830–833.
[14] C. Zhe *et al.*, "Speckle suppression by controlling the coherencein laser based projection systems," *J. Display Technol.*, vol. 11, no. 4, pp. 330–335, 2015.
[15] J. T. Oh, D. A. Zimnyakov, and G. G. Akchurin, "Speckle contrast measurements with changeable coherence length: The method of scattering media probing," in *Proc. Saratov Fall Meeting, Coherent Opt. Ordered Random Media II*, 2002, pp. 137–144.
[16] C. Zheng *et al.*, "All-fiber 30-μm core diameter Yb-doped pulse-pumped amplifier cascade generating 10 nm-bandwidth 545 kW peak power pulses all-fiber Yb-doped pulse-pumped amplifier cascade generating," *Laser Phys. Lett.*, vol. 9, no. 6, pp. 451–455, 2012.
[17] G. Gao *et al.*, "All-normal-dispersion fiber laser with NALM: Power scalability of the single-pulse regime," *Laser Phys. Lett.*, vol. 15, no. 3, 2018, Art. no. 035106.
[18] Y. Shen *et al.*, "Gain-phase modulation in chirped-pulse amplification," *Phys. Rev. A*, vol. 96, no. 4, 2017, Art. no. 043851.